




An integrated proteomic and metabolomic study to evaluate the effect of nucleus-cytoplasm interaction in a diploid citrus cybrid between sweet orange and lemon

Teresa Faddetta^{1,2} · Loredana Abbate³ · Giovanni Renzone⁴ · Antonio Palumbo Piccionello¹ · Antonella Maggio¹ · Elisabetta Oddo¹ · Andrea Scalonì⁴ · Anna Maria Puglia¹ · Giuseppe Gallo^{1,2} · Francesco Carimi³ · Sergio Fatta Del Bosco³ · Francesco Mercati³ 

Received: 1 June 2018 / Accepted: 10 October 2018 / Published online: 19 October 2018
© Springer Nature B.V. 2018

Abstract

Key message Our results provide a comprehensive overview how the alloplasmic condition might lead to a significant improvement in citrus plant breeding, developing varieties more adaptable to a wide range of conditions.

Abstract Citrus cybrids resulting from somatic hybridization hold great potential in plant improvement. They represent effective products resulting from the transfer of organelle-encoded traits into cultivated varieties. In these cases, the plant coordinated array of physiological, biochemical, and molecular functions remains the result of integration among different signals, which derive from the compartmentalized genomes of nucleus, plastids and mitochondria. To dissect the effects of genome rearrangement into cybrids, a multidisciplinary study was conducted on a diploid cybrid (C2N), resulting from a breeding program aimed to improve interesting agronomical traits for lemon, the parental cultivars ‘Valencia’ sweet orange (V) and ‘femminello’ lemon (F), and the corresponding somatic allotetraploid hybrid (V + F). In particular, a differential proteomic analysis, based on 2D-DIGE and MS procedures, was carried out on leaf proteomes of C2N, V, F and V + F, using the C2N proteome as pivotal condition. This investigation revealed differentially represented protein patterns that can be associated with genome rearrangement and cell compartment interplay. Interestingly, most of the up-regulated proteins in the cybrid are involved in crucial biological processes such as photosynthesis, energy production and stress tolerance response. The cybrid differential proteome pattern was concomitant with a general increase of leaf gas exchange and content of volatile organic compounds, highlighting a stimulation of specific pathways that can be related to observed plant performances. Our results contribute to a better understanding how the alloplasmic condition might lead to a substantial improvement in plant breeding, opening new opportunities to develop varieties more adaptable to a wide range of conditions.

Keywords *Citrus* spp. · Protoplast fusion · Cybrid · Proteomics · Volatile organic compounds · Stomatal conductance

Abbreviations

V Valencia sweet orange
F Femminello lemon
V + F Allotetraploid somatic hybrid
Valencia + femminello

C2N Femminello lemon cybrid
2D-DIGE Two-dimensional differential gel electrophoresis
MS Mass spectrometry
BLAST Basic local alignment search tool
KEGG Kyoto encyclopedia of genes and genomes
RCA Ribulose biphosphate carboxylase/oxygenase activase
PsbP Photosystem II oxygen-evolving enhancer protein 2
GAPCp Plastidial glyceraldehyde-3-phosphate dehydrogenase A
ATP Adenosine triphosphate
mMDH Mitochondrial malate dehydrogenase enzyme
GC/MS Gas chromatography/mass spectrometry

Teresa Faddetta and Loredana Abbate authors contributed equally to this work.

Electronic supplementary material The online version of this article (<https://doi.org/10.1007/s11103-018-0787-9>) contains supplementary material, which is available to authorized users.

✉ Francesco Mercati
francesco.mercati@ibbr.cnr.it

Extended author information available on the last page of the article

BVOC	Biogenic volatile organic compounds
PAL	Phenylalanine-ammonia lyase
PEG	Polyethylene glycol
RFLP	Restriction fragment length polymorphism
SSR	Simple sequence repeat
PCR	Polymerase chain reaction
IEF	Isoelectric focusing

Introduction

Citrus is the most economically important evergreen subtropical fruit crop in the world, with more than 9 million hectares grown and about 125 million tons of fruits produced in 2017 (FAO 2017; Navarro et al. 2015; Willer and Lernoud 2016). All citrus fruits are an essential source of vitamin C, contributing to the nutritional supply of humans, together with polyphenols and carotenoids. Conventional breeding in citrus is hindered by several biological barriers, such as sexual incompatibility, nucellar polyembryony, long juvenility, pollen and ovule sterility. Accordingly, most citrus cultivars derive from somatic mutations, which lead to a poor and narrow genetic diversity.

Biotechnological approaches circumvent these difficulties, improving breeding efficiency and expediting genetic improvement processes. Among the current strategies used to this purpose, somatic hybridization via protoplast fusion represents the most powerful method to overcome sexual barriers and to generate novel and unobtainable germplasm resources (Grosser and Gmitter 1990; Guo and Deng 2001; Fu et al. 2009; Eeckhaut et al. 2013; Guo et al. 2013; Tarwacka et al. 2013; Liu and Xia 2014). In the past two decades, a large number of intergeneric and interspecific citrus somatic hybrids has been obtained and used in scion and rootstock improvement; they have been used in breeding programs for specific agronomic traits, such as seedlessness and disease resistance (Cai et al. 2007; Fu et al. 2009, 2011; Grosser and Gmitter 2011; Dambier et al. 2011; Guo et al. 2013). Nevertheless, since most citrus cultivars are diploids, the resulting somatic hybrids are mainly allotetraploids, containing the complete nuclear genomes of both parents (Grosser et al. 2000). Unfortunately, the increased chromosome number in the hybrid and the incompatibility of genome recombination may influence the genetic integration of the desired traits into the cultivated varieties (Osborn et al. 2003); accordingly, tetraploidy has often been associated with several unfavourable agronomic traits. On this basis, the use of tetraploid varieties in commercial citrus orchards has found a very limited application. However, several diploid plants with morphology similar to the leaf-parent (non-embryogenic) have also been generated after somatic hybridization experiments (Grosser et al. 1996; Liu et al. 1999). Molecular characterization of these

leaf-parent-type plants revealed that they are diploid cybrids, which contain nuclear DNA genome of the leaf parent, and either mtDNA and cpDNA of the embryogenic callus/suspension parent or randomly inherited from both parental species (Moreira et al. 2000; Guo et al. 2004, 2006). In contrast to sexual hybridization, where the cytoplasmic genomes are maternally inherited, somatic hybridization generates novel nuclear-cytoplasmic combinations. Since higher plants features are genetically controlled by the interaction among nuclear, plastidial and mitochondrial genomes (Suzuki et al. 2012; Luo et al. 2013; Ng et al. 2014), the possibility of having new and original combinations of nuclei and organelles may have interesting applications in the creation of novel genotypes with potential agronomic values (Grosser et al. 1996; Guo et al. 2004, 2013; Cabasson et al. 2001; Xiao et al. 2014; Aleza et al. 2016; Fang et al. 2016; Omar et al. 2017). Plastids and mitochondria fulfil important metabolic functions that greatly affect plant growth and productivity. Many metabolic and developmental pathways involved in plant adaptation intersect within the plastid (Rolland et al. 2012), such as phytohormone- and lipid-centred processes and plant biotic defence. Likewise, heat tolerance, cytoplasmic male sterility and oxidative stress response (Jacoby et al. 2012) are controlled by mitochondria. The peculiar genetic structure of cybrids makes them the most appropriate candidates for studies on plant adaptive mechanisms and for the analysis of nuclear-cytoplasmic interactions.

Plant organellar replacement has been associated with changes in the corresponding transcriptome, metabolome, and proteome. Differential proteomic analysis is a powerful molecular approach for describing the rearrangement of the protein repertoire as a result of different genetic, endogenous and physiological factors (Zhao et al. 2013). Through the use of proteomic approaches, several advances have been made in understanding molecular events associated with plant physiology and function, e.g. mineral deficiency (Liang et al. 2013), abiotic stress response (Kosová et al. 2011; Zhang et al. 2013), disease tolerance (Rampitsch and Bykova 2012; Chetouhi et al. 2015), heavy metal hyperaccumulation (Visioli and Marmiroli 2013), flood tolerance (Komatsu et al. 2013) and fruit development/ripening (Palma et al. 2011).

A specific diploid cybrid was obtained by somatic hybridization experiments included in a selective breeding program aimed at improving citrus lemon quality traits (Abbate et al. 2012; Fatta Del Bosco et al. 2013) and enhancing resistance toward the most pathogenic fungal disease for lemon, i.e. “malsecco” caused by *Phoma tracheiphila* (Tusa et al. 2000; Scarano et al. 2003). In the present work, the selected cybrid was studied in comparison to its parents and the corresponding somatic allotetraploid hybrid by using integrated physiological, proteomic and metabolite-oriented analyses in order to highlight the role of the cytoplasmic genome

rearrangement and to provide useful information on protein expression associated with beneficial and/or valuable (pharmaceutical, nutraceutical and agronomic) traits.

Materials and methods

Plant materials

Citrus plants were obtained by somatic protoplast fusion between heterozygous inbred lines of ‘Valencia’ sweet orange (*Citrus sinensis* L. Osbeck) (V) and ‘femminello’ lemon (*Citrus limon* L. Burm) (F). The protoplasts were isolated from embryogenic callus of sweet orange and leave of lemon. The allotetraploid somatic hybrid ‘Valencia’ + ‘femminello’ (V + F) and the diploid ‘femminello’ lemon cybrid (C2N) were developed by the polyethylene glycol (PEG) method, as previously described (Tusa et al. 1990, 2000; Grosser et al. 1996; Abbate et al. 2012) and characterized by isozymes (Tusa et al. 1990), RFLP (Grosser et al. 1996) and SSR (Scarano et al. 2003). Here, five nuclear (nuSSR), eleven chloroplast (cpSSR) and nine mitochondrial (mtSSR) loci (Cheng et al. 2003, 2005; Jannati et al. 2009; Froelicher et al. 2011) (Online Resource 1: Table S1) were used to characterize the cytoplasmic background of investigated plants. DNA was extracted from young fresh leaves (Lodhi et al. 1994), and its quality and concentration was verified by a NanoDrop spectrophotometer (Thermo Scientific). PCR reactions were performed following the procedures reported in Mercati et al. (2013). The fragments were separated by capillary electrophoresis using an ABI PRISM 3500 Genetic Analyzer (Applied Biosystems).

Citrus cybrid, somatic hybrid and parental plants were grafted onto the same rootstock (*Citrus aurantium* L.) and subjected to identical, standard cultivation practices in the experimental field station of IBBR–CNR in Collesano, Palermo (Italy). The plant material was collected in June 2015. For all experiments, 30 healthy and fully-expanded leaves from the last finished sprouting branches were harvested. The effects of tree and branch position were minimized by random sampling. Leaves were collected at noon (under full sun) and immediately frozen in liquid nitrogen. Three different specimens for each genotype were analysed. Leaf samples were stored at -80°C until use.

Protein extraction

For each sample, whole protein extracts were obtained from 100 mg of collected leaves. Eight different extraction methods were tested, using the procedures described by Puglia et al. (1995) and Wang et al. (2006) with or without extensive modifications (Online Resource 2: Table S2). All the biomass samples were washed two times with 1 ml of

10 mM Tris–HCl pH 7.5, 5 mM EDTA, 1 mM DTT, 0.5 mM PMSF, 4 mg/ml leupeptin, 0.7 mg/ml pepstatin, 5 mg/ml benzamidin by vortexing, and then centrifuged ($15,000\times g$, 10 min, at 4°C). All the other pre-wash or wash steps (Table S2) were performed using 2 ml of solvents/buffers by vortexing and following centrifugation ($15,000\times g$, 4 min, at 4°C). Cells were disrupted by sonication on ice in 1 ml of extraction buffer (output control 4, 8×15 s, Vibra Cell, USA). All protein extracts were boiled for 5 min, and rapidly cooled down on ice for 15 min; then they were treated with DNase (100 $\mu\text{g/ml}$) and RNase (50 $\mu\text{g/ml}$) in ice, for 15 min. Cell debris and non-broken cells were separated by centrifugation ($15,000\times g$, for 15 min, at 4°C). In order to remove salts and low molecular mass contaminants, which may interfere with CyDye-labeling of proteins and their 2D-gel electrophoretic separation, extracts were dialyzed against distilled water (for 3 h, at 4°C) and/or treated with 1 vol of phenol/chloroform/isoamyl alcohol (25/24/1, v/v; Sigma-Aldrich) for 5 min at room temperature mixing by vortex. After centrifugation ($15,000\times g$, 5 min, at 4°C), they were recovered from interface and organic phases by discharging the aqueous phase. Finally, proteins were precipitated using one of the two methods reported in Table S2, at -20°C , overnight, and protein precipitate was recovered by centrifugation ($15,000\times g$, 10 min, at 4°C). Before resuspension, if needed, protein pellets were further washed with 1 ml of methanol and/or acetone, centrifuged ($15,000\times g$, 20 min, at 4°C), and then solved in 50–100 μl of isoelectric focusing (IEF) buffer (30 mM Tris pH 8.5, 7 M urea, 2 M thiourea, 4% w/v CHAPS, pH 8.4).

2D-differential in gel electrophoresis (2D-DIGE) and imaging

For Two-Dimensional Differential in Gel Electrophoresis (2D-DIGE) analysis, leaf proteins from three replicates for each genotype (i.e. V, F, V + F and C2N) were used. Protein samples were labelled for 2D-DIGE analysis using the CyDye™ DIGE minimal labeling kit (GE Healthcare, Sweden) as previously described (Palazzotto et al. 2015). In particular, after determination of protein concentration using Bradford reagent, 50 μg of each protein sample were labelled with 200 pmol of CyDye on ice, in the dark, for 30 min, performing dye-swapping to minimize dye-specific labeling effects according to manufacturer’s recommendations. Labelling reaction was quenched by the addition of 0.5 μl of 10 mM lysine; incubation was continued on ice for 10 min, in the dark. For IEF, DeStreak rehydration solution (GE Healthcare, Sweden) containing 0.5% v/v immobilized pH gradient (IPG) buffer (GE Healthcare, Sweden) and 20 mM DTT (Sigma, Australia) was added to each mix to reach a 340 μl final volume. IEF was performed as previously described (Palazzotto et al. 2015), using non-linear 3–10 pH

range, 18 cm IPG strips (GE Healthcare, Sweden) in an Ettan IPGphor III apparatus (GE Healthcare, Sweden). After IEF, IPG strips were incubated with an equilibration buffer (6 M urea, 30% v/v glycerol, 2% w/v SDS, and 0.05 M Tris-HCl, pH 6.8) containing 2% w/v DTE for 10 min. Protein thiol groups were then blocked by further incubation with equilibration buffer containing 2.5% w/v iodoacetamide. Focused proteins were then separated by using 12% SDS-PAGE, at 10 °C, in an Ettan Daltsix (GE Healthcare, Sweden) apparatus, with a maximum setting of 40 μ A per gel and 110 V. The obtained 2D-gels were digitalized by using Typhoon FLA 9500 instrument (GE Healthcare, Sweden) following manufacturer's instructions, and setting photomultiplier tube at 740, 600 and 700 V for Cy3, Cy5 and Cy2 channels, respectively. 2D-gel image analysis was performed using Image Master 2-D platinum (version 7.0) 2D-DIGE enabled software (GE Healthcare, Sweden), according to manufacturer's instructions. Protein spots showing at least 1.5-fold change in their normalized volume (increased for over-representation or decreased for down-representation), with a statistically significant ANOVA value ($P \leq 0.05$), were considered as differentially represented; they were selected for further mass spectrometry (MS) analysis for protein identification. To this aim, 2D-gels were also stained with ammoniacal silver, as described in Palazzotto et al. (2016). The relative protein abundance profiles of identified protein spots were illustrated through heatmap clustering by using the R package ggplot2 (<https://cran.r-project.org/web/packages/ggplot2/index.html>).

Protein identification by mass spectrometry

Protein spots were carefully cut from the gels, triturated, in gel-reduced with dithiothreitol, S-alkylated with iodoacetamide, and subsequently in-gel digested with trypsin (sequencing grade, Roche). Resulting digests were desalted by μ Zip-TipC₁₈ (Millipore) before nanoLC-ESI-LIT-MS/MS analysis (Gallo et al. 2016) using a LTQ XL mass spectrometer (ThermoFisher, USA) equipped with a Proxeon nanospray source connected to an Easy-nanoLC (ThermoFisher). Peptides were resolved on an Easy C₁₈ column (100 mm \times 0.075 mm, 3 μ m) (Proxeon, Denmark). Mobile phases (LC-MS grade) were 0.1% v/v formic acid (solvent A) and 0.1% v/v formic acid in acetonitrile (solvent B), running at a total flow rate of 300 nl/min. A linear gradient was initiated 20 min after sample loading; solvent B ramped from 5 to 35% over 10 min, and from 35 to 95% over 2 min. Spectra were acquired in the range of m/z 400–2000. Peptides were analysed under collision-induced dissociation data-dependent product ion scanning procedure, enabling dynamic exclusion (repeat count 1 and exclusion duration 60 s) over the three most abundant ions.

Mass isolation window and collision energy were set to m/z 3 and 35%, respectively.

Raw data from nanoLC-ESI-LIT-MS/MS analysis were searched by MASCOT search engine (version 2.2, Matrix Science, UK) against an updated NCBI non-redundant database (October 2015) with the aim to identify proteins from gel spots. Database searching was performed by using Cys carbamidomethylation and Met oxidation as fixed and variable protein modifications, respectively, a mass tolerance value of 1.8 Da for precursor ion and 0.8 Da for MS/MS fragments, trypsin as proteolytic enzyme, and a missed cleavage maximum value of 2. Other MASCOT parameters were kept as default. Protein candidates assigned according to at least two sequenced peptides with an individual peptide expectation value < 0.05 (corresponding to a confidence level for peptide identification $> 95\%$) were considered confidently identified. Definitive peptide assignment was always associated with manual spectra visualization and verification.

GC/MS analysis

Freshly collected leaves (around 500 mg) were cut and placed in a special vial for headspace. The sample preparation was performed with a MultiPurpose Sampler MPS apparatus (Gerstel, Mulheim an der Ruhr, Germany) equipped with a cooled agitator. The temperature of the syringe was set to 40 °C, flush time 30 s; the sample was heated to 40 °C, for 10 min, under stirring (speed 250 rpm).

The headspace analysis was performed in an Agilent 7000C Triple Quadrupole GC/MS system, fitted with a fused silica Agilent HP-5 capillary column (10 m \times 0.25 mm i.d.; 0.25 μ m film thickness), coupled to an Agilent Mass Selective Detector MSD 5973; ionization voltage 70 eV; electron multiplier energy 2000 V. Helium was the carrier gas (1 ml/min). Column temperature was initially kept at 40 °C for 5 min, then gradually increased to 250 °C, at a rate of 2 °C/min, held for 15 min, and finally raised to 270 °C, at 10 °C/min. Transfer line temperature was 295 °C. Most constituents were identified by gas chromatography by comparison of their retention indices (I) with those from the literature (Hijaz et al. 2016) or with those of standard compounds. The retention indices were determined in relation to a homologous series of *n*-alkanes (C₈–C₃₂) under the same operating conditions. Further identification was made by comparison of their mass spectra with counterparts stored in NIST 02 and Wiley 275 libraries or with mass spectra from the literature (Sparkman 2005) and from a homemade library. Component relative concentrations were calculated based on GC peak areas, without using correction factors.

Polyphenol extraction

Freshly collected leaves (around 50 g) were lyophilized for 24 h and then extracted with 96% v/v ethanol in a Büchi B-811 extraction system, for 1 h. In order to remove lipophilic metabolites, ethanolic extracts were dried and fractionated with a Biotage Isolera One automatic MPLC system, equipped with a cartridge SNAP Ultra C18 (HP Sphere C18 25 μm , 120 g). Mobile phases were water (solvent A) and methanol (solvent B), which were used in a linear gradient from 0 to 100% of solvent B; eluates were monitored with an UV detector in the range 200–400 nm. Fractions containing polyphenols were lyophilized, weighted and stored at 4 °C until analysis. Samples for further HPLC analysis were prepared dissolving 1 mg of the obtained extract with methanol (1 ml).

Reversed-phase HPLC–ESI–Q-TOF–MS/MS analysis of polyphenols

HPLC analysis was performed with an 1260 Infinity system (Agilent) equipped with a reversed-phase Phenomenex Luna C18 (2) column (150 \times 4.6 mm, particle size 3 μm) bearing a Phenomenex C18 security guard column (4 \times 3 mm). The flow-rate was 0.5 ml/min and the column temperature was set to 30 °C. The eluents were 0.1% v/v formic acid (solvent A) and 0.1% v/v formic acid in acetonitrile (solvent B). The following gradient was used: 0–5 min, 5% solvent B isocratic; 5–15 min, linear gradient from 5 to 15% solvent B; 15–20 min, 15% solvent B isocratic; 20–25 min, linear gradient from 15 to 30% solvent B; 25–35 min, 30% solvent B isocratic; 35–45 min, washing and reconditioning of the column. Injection volume was 25 μl . The eluate was monitored through MS by measuring total ion current. Mass spectra were obtained on an Agilent 6540 UHD accurate-mass Q-TOF spectrometer equipped with a Dual AJS ESI source working in negative mode. N_2 was used as desolvation gas at 300 °C and a flow rate of 8 l/min. The nebulizer was set to 45 psig. The sheath gas temperature was set at 400 °C and a flow of 12 l/min. A potential of 2.6 kV was applied to the capillary for negative ion mode. The fragmentor was set to 75 V. MS spectra were recorded in the range of m/z 150–1000; MS/MS spectra were recorded in negative mode with a collision energy of 50 V.

Leaf gas exchange measurements

Measurements of net photosynthesis (A , $\mu\text{mol m}^{-2} \text{s}^{-1}$), leaf conductance (g_s , $\text{mmol m}^{-2} \text{s}^{-1}$), intercellular CO_2 concentration (C_i , $\mu\text{mol m}^{-1}$) and the ratio between internal and external CO_2 concentration (C_i/C_a) were carried out using a portable infra-red gas analyzer (HCM-1000 Walz, Germany) under ambient light and CO_2 conditions. Measurements

were taken on five fully expanded mature leaves of three plants per genotype, between 09:30 and 11:30 h am. The incident photosynthetic photon flux density (PPFD) was 1500 $\mu\text{mol m}^{-2} \text{s}^{-1}$, cuvette air temperature ranged from 28.2 to 30.1 °C and reference CO_2 concentration was between 387 and 407 $\mu\text{mol mol}^{-1}$. Gas exchange data were reported on a leaf area basis. The data were analysed by one-way ANOVA comparing among studied genotypes, and mean values were separated by Tukey's honest significant difference (HSD) test ($P < 0.05$).

Results

Preliminary investigations towards comparative analyses

Molecular characterization by microsatellites confirmed that V + F and C2N were the hybrid and cybrid, respectively (Online Resource 3: Table S3), as reported also in previous studies (Grosser et al. 1996; Scarano et al. 2003). In addition, cytoplasmic markers distinguished parental genomes, highlighting that the chloroplasts and mitochondria were inherited from both parents in V + F and C2N genotypes. Eight protein extraction procedures based on existing methods (Puglia et al. 1995; Wang et al. 2006) with or without extensive modifications were also comparatively evaluated (Table S2), to optimize a suitable protocol for further proteomic analysis based on 2D-DIGE technology and compatible with subsequent silver staining for spot picking and MS-based protein identification. According to the experimental evidences described in Online Resource 4 (Fig. S1) and Online Resource 5 (Fig. S2), method n. 3 resulted the most effective and, therefore, was chosen to prepare leaf protein extracts for subsequent comparative proteomic analysis.

Comparative analysis of the leaf proteome from different citrus cultivars

In order to identify up- or down-regulated molecular pathways in the C2N genotype, a differential proteomic analysis was performed, combining 2D-DIGE and nanoLC–ESI–LIT–MS/MS experiments. Protein extracts from leaf biomass samples of C2N, V + F and the parental cultivars F and V were comparatively analysed, with the former used as pivotal condition. In order to obtain a simplified representation of the quantitative behaviour of all proteome patterns a heatmap clustering was generated using the mean abundance values of a total of 52 protein species with a P -value < 0.05 (ANOVA test) (Online Resource 6: Fig. S3). This analysis revealed three major clusters highlighting a distinct proteome profile of C2N genotype, clearly distinguishing it from its parents and the

resultant allotetraploid somatic hybrid. Among the above described group of protein spots, those showing differential abundance in the C2N proteome were selected for protein identification as reported in Table 1 and in Online Resource 7 (Fig. S4). In particular, taking into count that some of the spots were shared between the three datasets of differentially represented protein species resulting from the three paired comparisons (C2N vs. F, C2N vs. C, and C2N vs. V + F), a total of 20 spots were univocally assigned to a protein identification with the following abundance profile: (i) 18 spots over-represented in C2N in comparison with F; (ii) 15 over- and 1 down-represented in the C2N in comparison with V; (iii) 17 over- and 1 down-represented in the C2N in comparison with V + F (Table 1). Based on putative function deduced after BLAST interrogations against KEGG2 database (Kanehisa and Goto 2000), the identified protein species were clustered into 6 functional groups, which included carbon (20%), energy (20%), nucleotide (15%), amino acid (10%) and protein (10%) metabolism, and components with unknown function (20%) (Table 1). Interestingly, 9 out of 20 identified proteins were assigned to cytoplasmic organelles, i.e. mitochondria and chloroplasts. This analysis definitely revealed that the C2N proteome has a peculiar pattern, which highly differs from that of both parents and somatic hybrid. Indeed, except for a component involved in photosynthesis (spot 25), 2 species related to protein metabolism (spots 26 and 35) and 4 species with unknown function (spots 15, 17, 31 and 32), the other differentially represented components were up-regulated in C2N genotype, when compared to parents (Table 1; Online Resource 6: Fig. S3). Similarly, differentially represented proteins in the C2N genotype were always over-represented when compared to the allotetraploid somatic hybrid, with the exception of 3 (spot 31, 32 and 35) out of the above mentioned components (Table 1, Online Resource 6: Fig. S3). The overall protein accumulation pattern in C2N suggested a general induction of metabolic and molecular processes therein, which thereof implies a cybrid heterosis compared to its parents and the corresponding allotetraploid somatic hybrid. It is noteworthy that 8 proteins over-expressed in the C2N proteome profile, when compared to the V + F allotetraploid hybrid, are involved in carbon and energy metabolism (Table 1, Online Resource 6: Fig. S3). Among them, worth mentioning are: (i) ribulose biphosphate carboxylase/oxygenase (rubisco) activase (RCA, spot 9), a key enzyme involved in photosynthesis and CO₂ assimilation (Portis et al. 2008); (ii) photosystem II oxygen-evolving enhancer protein 2 (PsbP, spot 25); (iii) the plastidial glyceraldehyde-3-phosphate dehydrogenase A (GAPCp, spot 34), a key glycolytic enzyme; (iv) two subunits (δ and ϵ) of the ATP synthase complex (spot 24 and 29); (v) the mitochondrial malate dehydrogenase enzyme (mMDH,

spot 10), involved in tricarboxylic acid (TCA) cycle. An accumulation pattern was also observed for peroxidase 3-like protein (spot 8) and two different 14-3-3-like proteins (spot 19 and 20).

Analysis of volatile and phenolic compounds

Leaf headspace composition from each sample was evaluated through GC/MS analysis (Hijaz et al. 2016). Fourteen volatile compounds were identified (Table 2); among them, monoterpene hydrocarbons were the main class, in which limonene was observed as the most abundant volatile constituent in C2N and V + F, while sabinene was the main metabolite in femminello and Valencia (Table 2; Online Resource 8: Table S4). Interestingly, normalizing with the amount of limonene identified in the Valencia genotype, femminello, V + F and C2N showed 2.9-, 6.9- and 11.2-fold higher production, respectively. Similarly, the analysis for sabinene showed a ratio of 1:2.5:3.3:3.4 for V, F, V + F and C2N, respectively (Online Resource 8: Table S4). The distribution of sabinene and limonene content in each genotype and the corresponding ratio are reported in Fig. 1.

Concerning the corresponding polyphenolic profile, the ethanolic extracts from lyophilized leaves were also analysed; they corresponded to 2.42, 6.38, 1.33 and 0.69% w/ leaf FW for V, F, V + F and C2N, respectively. A qualitative characterization of polyphenolic derivatives was performed through HPLC–ESI–Q–TOF–MS/MS (Brito et al. 2014). Fifteen compounds were detected, mainly diglycosylated flavones and flavanones (Table 3). Although a lower amount of the ethanolic extract was measured for genotypes obtained by protoplast fusion (V + F and C2N), when compared to that of parents (V and F), the former ones presented the most variable profile from a qualitative point of view. In addition, V + F hybrid showed a quite lower flavones/flavanones ratio than the other three genotypes.

Gas exchange

To assess the effects of the cytoplasmic genome rearrangement into C2N genotype and to validate the above-mentioned biochemical evidences according to a cumulative physiological perspective, leaf gas exchange and net photosynthesis were also evaluated in all genotypes. The most relevant difference was found in the stomatal conductance of the regenerated C2N plants, which was significantly higher than that of the other genotypes (Fig. 2a). Indeed, g_s in C2N leaves was more than twice that of the leaf parent F and 60% greater than the somatic hybrid (V + F). Correspondingly, internal CO₂ concentration (C_i) was highest in C2N (274 μ bar), 40% greater than in V + F, and the lowest C_i was measured in F (144 μ bar) (Fig. 2b). The [CO₂] increase in C2N resulted in a higher rate of photosynthesis

Table 1 Differentially represented proteins in C2N as deduced by combined 2D-DIGE and nanoLC-ESI-LIT-MS/MS analyses

Spot	Protein name	Source	NCBI code	Mascot score	Unique peptides	Sequence coverage %	KEGG homologue ¹	KEGG ontology ¹	Cellular process/metabolic pathways ²	C2N versus F ³	C2N versus V ³	C2N versus V + F ³
7	Hypothetical protein CICLE_v10008224mg	<i>C. clementina</i>	gil567916650	288	5	15.3	Hypothetical protein-aspartate aminotransferase, chloroplastic	K00811	Amino acid metabolism/biosynthesis of amino acids; isoquinoline alkaloid biosynthesis	2.8	1.6	3.0
1	Hypothetical protein CICLE_v10018965mg	<i>C. clementina</i>	gil567901962	451	6	11.0	5-Methyltetrahydropteroyl-triglutamate-homocysteine methyltransferase	K00549	Amino acid metabolism/biosynthesis of amino acids; selenocompound metabolism	3.1	1.9	2.1
34	Glyceraldehyde-3-phosphate dehydrogenase A, chloroplastic-like	<i>C. sinensis</i>	gil568829274	366	5	16.1	Glyceraldehyde-3-phosphate dehydrogenase A, chloroplastic-like	K05298	Carbon metabolism/ carbon fixation in photosynthetic organisms	3.6	5.7	2

Table 1 (continued)

Spot	Protein name	Source	NCBI code	Mascot score	Unique peptides	Sequence coverage %	KEGG homologue ¹	KEGG ontology ¹	Cellular process/metabolic pathways ²	C2N versus F ³	C2N versus V ³	C2N versus V + F ³
23	Pectinesterase 3	<i>C. sinensis</i>	gi57014097	114	2	4.1	Pectinesterase	K01051	Carbon metabolism/pentose and gluconate interconversions; starch and sucrose metabolism	6.2	2.4	4.3
18	Hypothetical protein CICLE_v10026210mg	<i>C. clementina</i>	gi567867079	311	5	28.6	Xyloglucan:xyloglucosyl transferase	K08235	Carbon metabolism/xyloglucan metabolism	7.9	3.1	7.2
10	Malate dehydrogenase, mitochondrial	<i>Fragaria X ananassa</i>	gi24638017	200	3	12.4	Malate dehydrogenase, mitochondrial	K00026	Carbon metabolism/TCA cycle	1.7	7.0	2.5
24	ATP synthase delta chain, chloroplastic-like	<i>C. sinensis</i>	gi568838468	142	2	12.0	F-type H ⁺ -transporting ATPase subunit delta	K02113	Energy metabolism/oxidative phosphorylation; photosynthesis	7.8	4.1	4.7
29	ATP synthase CF1 epsilon subunit	<i>C. sinensis</i>	gi114329662	131	2	18.8	ATP synthase CF1 epsilon subunit	K02114	Energy metabolism/oxidative phosphorylation; photosynthesis	7.8	3.1	7.6

Table 1 (continued)

Spot	Protein name	Source	NCBI code	Mascot score	Unique peptides	Sequence coverage %	KEGG homologue ¹	KEGG ontology ¹	Cellular process/metabolic pathways ²	C2N versus F ³	C2N versus V ³	C2N versus V + F ³
9	Hypothetical protein C1SIN_1g012383mg	<i>C. sinensis</i>	gil641850272	466	6	21.9	Ribulose biphosphate carboxylase/oxygenase activase 1, chloroplastic-like	–	Energy metabolism/ photosynthesis	1.5	4.0	2.5
25	Hypothetical protein CICLE_v10032502mg	<i>C. clementina</i>	gil567889122	199	4	17.4	Photosystem II oxygen-evolving enhancer protein 2	K02717	Energy metabolism/ photosynthesis	3.9	–1.2	2.0
19	14-3-3-like protein D-like isoform X1	<i>C. sinensis</i>	gil568829418	443	7	37.6	14-3-3-like protein D-like	K06630	Nucleotide metabolism/ DNA repair and recombination proteins	4.9	1.6	3.0
20	Hypothetical protein CICLE_v10029087mg	<i>C. clementina</i>	gil567862314	279	4	23.0	14-3-3 protein epsilon	K06630	Nucleotide metabolism/ DNA repair and recombination proteins	7.5	1.5	5.2
28	Bis(5'-adenosyl)-triphosphatase-like	<i>C. sinensis</i>	gil568873692	466	6	23.6	Bis(5'-adenosyl)-triphosphatase-like	K01522	Nucleotide metabolism/ purine metabolism	1.5	4.7	1.9
35	28 kDa ribonucleoprotein, chloroplastic-like	<i>C. sinensis</i>	gil568846150	256	4	16.5	Ribonucleoprotein, chloroplastic-like	–	Protein metabolism/ ribosome biogenesis	1.2	1.9	1

Table 1 (continued)

Spot	Protein name	Source	NCBI code	Mascot score	Unique peptides	Sequence coverage %	KEGG homologue ¹	KEGG ontology ¹	Cellular process/metabolic pathway ²	C2N versus F ³	C2N versus V ³	C2N versus V + F ³
26	30S ribosomal protein 2, chloroplast-like	<i>C. sinensis</i>	gi568858613	106	2	8.1	30S ribosomal protein 2, chloroplast-like	K13126	Protein metabolism/ RNA transport; mRNA surveillance pathway; RNA degradation	6.3	1.1	2.5
8	Peroxidase 3-like	<i>C. sinensis</i>	gi568852537	367	5	22.8	Peroxidase 3-like	K00430	Secondary metabolism/phenylpropanoid biosynthesis	1.8	4.3	2.8
15	Aspartic proteinase CDR1-like	<i>C. sinensis</i>	gi568862537	242	4	14.7	Aspartic proteinase CDR1-like	-	Unknown	4.7	1.6	1.9
17	Agglutinin-2-like	<i>C. sinensis</i>	gi568,885314	247	3	15.7	Agglutinin-2-like	-	Unknown	5.9	1.3	3.5
31	Aspartic proteinase CDR1-like	<i>C. sinensis</i>	gi568862533	260	4	14.3	Aspartic proteinase CDR1-like	-	Unknown	2.2	1.2	1.1
32	Hypothetical protein CICLE_v10006096mg	<i>C. clementina</i>	gi567852607	373	7	53.4	Hypothetical protein	-	Unknown	1.4	-5.2	-2.3

¹Results are obtained from BLAST interrogations against KEGG2 database by using protein amino acid sequence associated to the corresponding NCBI code

²Function was predicted according to KEGG database

³Abundance values are reported as fold change according to 2D-DIGE analysis. Positive and negative values stand for over- and down-representation in C2N, with respect to the other genotypes, respectively

Table 2 Composition of the leaf headspace and relative amount (peak area %) of 14 volatile compounds detected in each analysed genotype

	RT	KI	C2N	F	V+F	V
Monoterpenes hydrocarbons			99.31	79.89	98.86	90.99
Alpha-pinene	10.697	933	1.77	2.39	1.16	2.42
Alpha-fenchene	11.647	949	1.7	1.88	0.62	
Sabinene	13.396	974	30.75	42.75	37.38	51.14
ND	14.846	992	0.69	0.48	1.1	
Delta-3-carene	15.895	1007			2.74	
o-Cymene	16.995	1024	2.38	1.72	5.68	
Limonene	17.195	1027	59.56	29.21	46.29	29.99
E-beta-ocymene	18.845	1052	0.62	0.52		1.81
Gamma-terpinene	19.445	1060	0.64		2.68	3.52
Meta-cymene	21.594	1087	1.2	0.94	1.21	2.11
Other compounds						2.94
<i>n</i> -Nonanal	22.944	1105				2.94
Sesquiterpenes hydrocarbons			0.69	1.69	0.6	3.74
2-epi-alpha-funebrene	42.088	1388				1.27
Alpha-cis-bergamotene	43.588	1411	0.69	1.69	0.6	1.26
ND	46.337	1457				1.21
Total			100	81.58	99.46	98

Bold values indicate the amounts for each class of volatile compound and the total amount detected in the samples analysed

RT retention time, KI Kovats index, ND not determined

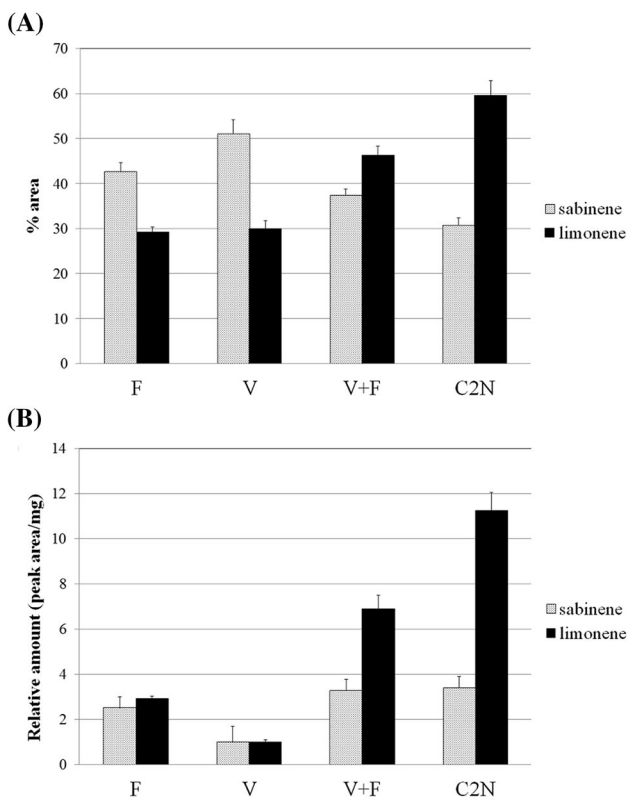


Fig. 1 a Distribution of principal metabolites (sabinene and limonene) in the four genotypes reported in this study, as deduced by GC/MS leaf's headspace analysis. The values are expressed in peak area %. b Relative amount (peak area/mg of leaf) of principal metabolites (sabinene and limonene) in femminello (F), V+F and C2N, as normalized to that of Valencia (V) (see Online Resource 6: Table S4)

(A) therein, when compared to the other genotypes (Fig. 2c), though this increase was not significant, and the lowest average value of A ($2.8 \mu\text{mol m}^{-2} \text{s}^{-1}$) was found in the F parent (Fig. 2c). Finally, we also evaluated the ratio between internal and external CO_2 concentration (C_i/C_a), which represents the balance between diffusion of CO_2 into the leaf and controlled by photosynthetic reactions (Ehleringer and Cerling 1995). The C2N genotype showed the greatest value of C_i/C_a , significantly higher than that of F and V+F genotypes (Fig. 2d).

Discussion

The generation of new nuclear-cytoplasmic combinations following cybridization is an important tool plant improvement that can also inform understanding of cyto-nuclear evolutionary dynamics (Greiner and Bock 2013). Indeed, since the nucleus encodes organelle-destined proteins for the control of subcellular districts and, in return, organelles send signals to the nucleus to coordinate nuclear and organelle activities (Woodson and Chory 2008), the cybrids obtained from somatic hybridization may represent a new technological tool for transferring organelle-encoded traits to cultivars. It is well known that somatic hybridization often results in novel mitochondrial and/or chloroplast genome arrangements (Belliard et al. 1979; Vedel et al. 1986; Dambier et al. 2011; Aleza et al. 2016; Fatta Del Bosco et al. 2017). Therefore, protoplast fusion leads to *de novo* nuclear

Table 3 Composition of the ethanolic extract from the leaves of each genotype

Compound	RT	ESI ⁻ [M-H] ⁻ (m/z)	Aglycon [M-H] ⁻ (m/z)	Phenolic structure	Area %			
					C2N	F	V+F	V
1	27.31 ± 0.03	447.0979	ND	ND	1.32	–	–	–
2	28.26 ± 0.02	595.1664	Eriodictyol 287.0552	Flavanone	–	–	15.29	–
3	28.43 ± 0.06	593.1570	Luteolin 285.0441	Flavone	–	15.59	–	4.55
4	28.54 ± 0.03	593.1510	Luteolin 285.0425	Flavone	33.74	–	7.69	1.96
5	28.81 ± 0.01	595.1664	Eriodictyol 287.0552	Flavanone	8.19	12.03	16.78	–
6	28.93 ± 0.03	593.1510	Luteolin 285.0426	Flavone	21.36	51.92	11.29	14.36
7	29.07 ± 0.02	431.0984	Apigenin ^b 283.0624	Flavone	1.62	–	1.79	–
8	29.39 ± 0.03	577.1606	ND	ND	–	2.93	–	–
9	29.63 ± 0.04	461.1090	Diosmetin ^b 298.0518	Flavone	–	–	4.50	–
10 ^a	29.66 ± 0.03	577.1614 607.1726	ND	ND	0.94	–	–	5.23
11 ^a	29.84 ± 0.08	577.1622 607.1726	ND	ND	2.48	–	3.18	1.84
12	29.99 ± 0.02	577.1612	Apigenin 269.0476	Flavone	7.06	10.44	5.99	10.55
13	30.14 ± 0.04	607.1719	Diosmetin 299.0585	Flavone	12.13	7.09	7.20	9.85
14	30.32 ± 0.03	607.1724	Diosmetin 299.0585	Flavone	11.16	–	11.78	18.77
15	30.61 ± 0.02	609.1887	Hesperetin 301.0740	Flavanone	–	–	14.49	32.88
				% Flavones	87.1	85.0	50.2	60.04
				% Flavanones	8.2	12.0	46.6	32.9

RT retention time, ND not determined

^aCo-elution of two different compounds

^bC-glucoside

and cytoplasmic genome combinations and to fertile and functional hybrid development (Tusa et al. 2000; Dambier et al. 2011; Xiao et al. 2014; Fang et al. 2016).

The present study has been conducted in attempt to advance our understanding of the role that cybridization plays in citrus breeding. Different studies examined the effect of cybridization on citrus phenotype, including changes to leaf volatile compounds (Fanciullino et al. 2005), fruit quality (Bassene et al. 2008) and organoleptic characteristics (Satpute et al. 2015), resistance to citrus “malsecco” disease caused by *Phoma tracheiphila* (Tusa et al. 2000), alteration in photosynthesis and stress resistance (Wang et al. 2010), altered gene expression related to floral organ development (Zheng et al. 2012), modifications of carbohydrate metabolism pathway and mitochondrial proteins in a male sterile cybrid (Zheng et al. 2014). A previous study (Bassene et al. 2011) reported a genome-wide gene expression analysis in leaves of a citrus cybrid and established that mitochondrial replacement affected the expression of different nuclear genes, including particularly genes predicted to be involved in mitochondrial retrograde signaling.

In this study, we have originally investigated the object of a plant cybridization process by using an integrated approach, which allowed comparatively evaluating at molecular and physiological level a citrus diploid cybrid isolated through a selective breeding program (Tusa et al. 2000; Scarano et al. 2003; Abbate et al. 2012; Fatta del Bosco

et al. 2013), its corresponding parents and an allotetraploid somatic hybrid obtained from the same interspecific fusion combination.

With the aim of elucidating molecular and metabolic pathways differentially regulated in the leaves of selected genotypes we performed a comparative proteomic analysis. Firstly, we established a method for protein extraction suitable for 2D-DIGE analysis. *Citrus* leaf tissue contains low amounts of proteins and high amounts of other components, such as lipids, organic acids and phenols, which vary in a specie-specific way and which may interfere with subsequent protein separation and analysis (Saravanan and Rose 2004; Audrius and Andrew 2005; Wang et al. 2006). Therefore, an *ad hoc* protocol was necessary. On a whole, our testing revealed that three key steps are crucial for protein recovery and removal of interfering compounds from citrus leaves: (i) three washing treatments using organic solvents, (ii) sonication in a SDS-containing buffer, with subsequent phenol/chloroform/isoamyl alcohol treatment; (iii) protein precipitation by methanol/ammonium acetate. Thus, we successfully identified 20 differentially represented proteins in the C2N genotype, nine of which are products of mitochondrial and chloroplast genomes. Hierarchical cluster analysis according to protein expression patterns showed a clear separation between C2N and other studied genotypes, underlining a private cluster for cybrid fully detached from both its parents and the somatic

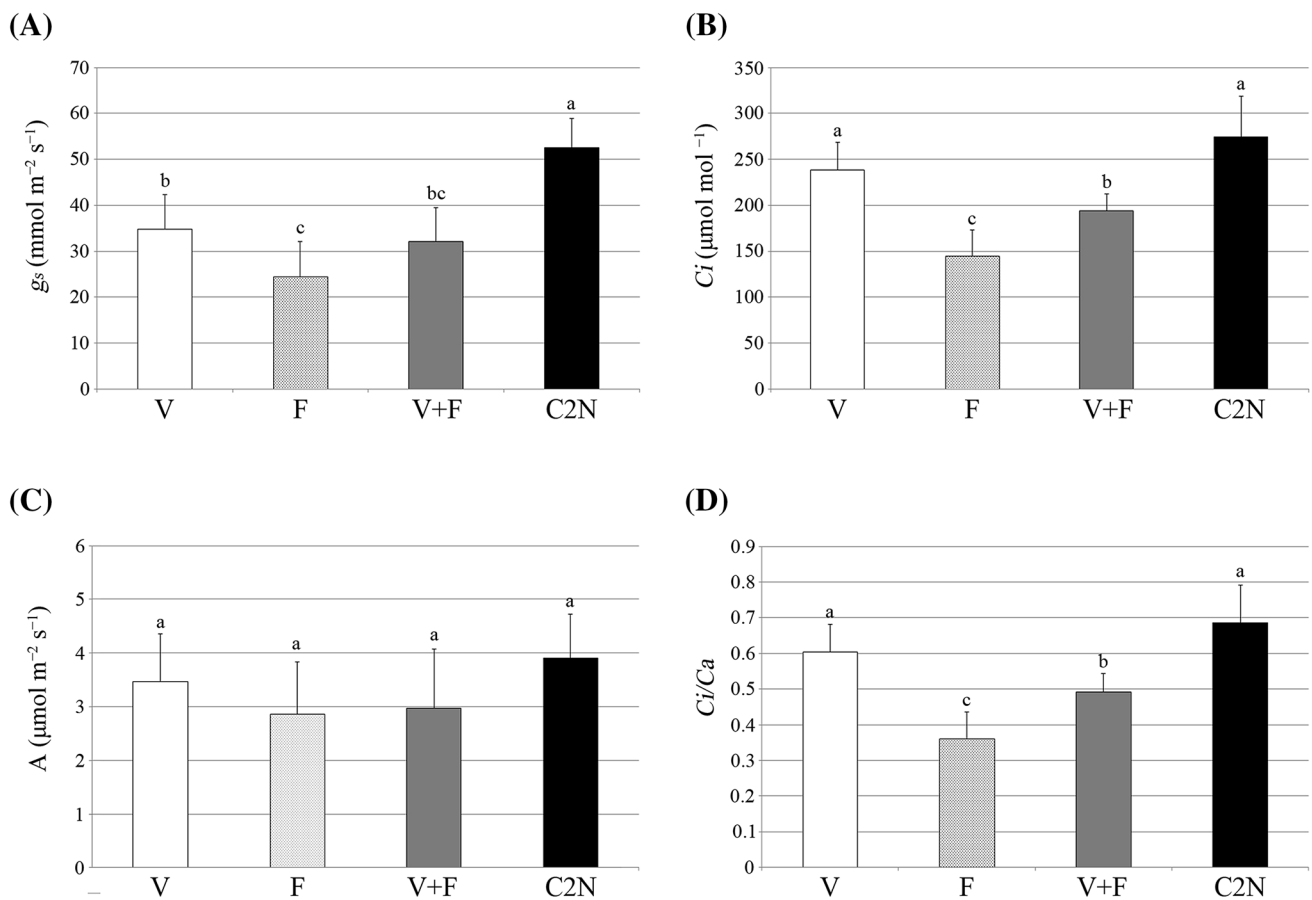


Fig. 2 Leaf gas exchange parameters. **a** Stomatal conductance to water vapour (g_s); **b** intercellular CO_2 concentration (C_i); **c** photosynthetic rate (A); **d** C_i/C_a ratio measured in the studied samples.

Values represent average measurements \pm SD. Bars sharing the same letter are not significantly different according to Tukey's HSD test ($P < 0.05$)

hybrid. Overall, our differential proteomic analysis suggests improved capabilities in terms of processes related to photosynthesis, energy metabolism and stress tolerance of the citrus cybrid, when compared to parental and somatic tetraploid hybrid genotypes as consequence of the improvement of the following molecular and biochemical processes: (i) CO_2 assimilation due to RCA activity (Crafts-Brandner and Salvucci 2000; Pollock et al. 2003; Salvucci 2008; Hozain et al. 2010); (ii) light-driven oxidation of water to molecular oxygen based on the augmented levels of PsbP—which plays a crucial role in enhancing O_2 generation in the oxygen-evolving complex of photosystem II (Roose et al. 2010); (iii) glycolytic capability as inferred by the augmented levels of GAPCp—an important connector between glycolysis and serine biosynthesis, ammonium assimilation and γ -aminobutyrate metabolism (Anoman et al. 2015) which has also a role in plant development (Muñoz-Bertomeu et al. 2010, 2011); (iv) reduced cofactor and ATP biosynthesis, as inferred by the augmented levels of the mMDH TCA cycle enzyme (Alqurashi et al. 2016) and chloroplastic ATP synthase complex components,

which may have also a beneficial role in energetic homeostasis in consequence of biotic or abiotic stresses (Yamori et al. 2011; Rott et al. 2011; Liu et al. 2014).

On the other hand, other proteins showing increased levels in cybrid leaves, such as 14-3-3-like proteins, have already been described as ubiquitous regulators (DeLille et al. 2001) which act in the cytoplasm (Bihn et al. 1997), in the chloroplast (Sehnke and Ferl 2000), in the nucleus (Bihn et al. 1997) and in mitochondria (Sehnke et al. 2000) completing signal transduction processes in many critical physiological pathways such as: nitrogen and carbon assimilation pathways (Sehnke et al. 2000); plant cell turgor pressure (Korthout and Boer 1994; Oecking et al. 1994); the activity of the enzymes starch synthase (Sehnke et al. 2001), glutamic acid synthase, F_1 ATP synthase, ascorbate peroxidase, and O-methyl transferase (Finnie et al. 1999).

Although further studies are needed to verify the hypotheses of beneficial effects on different physiological aspects of the activated pathways, the evidences here obtained through biochemical and physiological (see below) experiments are suggestive of the main molecular and macroscopic

mechanisms underlying the peculiar C2N behaviour. In this context, it has to be considered that plants produce a wide spectrum of biogenic volatile organic compounds (BVOCs), such as limonene, in various tissues; their emission varies widely depending on the species, organ, developmental stage and environmental conditions. BVOCs have important roles in plant adaptation and communication. For example, BVOCs have been reported to face the negative effects of biotic/abiotic stresses in an unanticipated, new mode of defence (Holopainen and Gershenzon 2010). In this light, it is noteworthy that a correlation between photosynthetic capability and terpene biosynthesis was already established (Penuelas and Munne-Bosch 2005; Loreto and Schnitzler 2010; Tezara et al. 2014). Our results demonstrate a higher production of limonene in C2N, when compared to that of parent and somatic hybrid genotypes. Since terpene production in the leaf was already associated with photosynthetic parameters, and a high photosynthetic capacity was related to high terpene content (Tezara et al. 2014), the higher concentration of limonene observed in the cybrid was here hypothetically related to its improved photosynthetic capacity and to its tolerance to stresses, based on proteomic assessment. Indeed, isoprenoids can improve plasticity in photo-protection and can help plants to survive under adverse climatic conditions. The protective role of some isoprenoids under non-photorespiratory conditions and their location in chloroplasts further underline their role in photoprotection and stress tolerance (Penuelas and Llusà 2002). Accordingly, these compounds might be of particular relevance in plant adaptation under adverse climatic conditions; thus, a comparative evaluation of their concentration may be useful in order to identify plants with a selective advantage for growing in contrasting habitats.

The hypothesized improved photosynthetic capability of the citrus cybrid, as based on proteomic experiments, was further assayed by dedicated physiological measurements, which were also performed in comparison with V, F and V + F genotypes. In this context, it is generally accepted that stomatal conductance (g_s) is an important factor controlling photosynthetic rate and related with the required mesophyll $[CO_2]$, maintaining the C_i/C_a ratio at a constant value (Wong et al. 1979; Sharkey and Raschke 1981; Kusumi et al. 2012). A high C_i/C_a ratio associated to greater net photosynthesis (A) was recorded in the C2N genotype, suggesting that the higher assimilation rates were due to greater g_s , which can enhance CO_2 diffusion into leaf and chloroplasts (Kusumi et al. 2012). A low value of C_i/C_a ratio, on the other hand, can result from low g_s levels, high photosynthetic capacity per unit leaf area, or a combination of both factors (Farquhar et al. 1989; Condon et al. 2004; Miner et al. 2017). High leaf stomatal conductance not only allows greater diffusion of CO_2 within the leaf, but allows high levels

of evapotranspiration that lower leaf temperature under well-watered conditions. Cooler leaves avoid the effects of high temperature on the activity of enzymes involved in carbon fixation and reduce photorespiration. When leaf temperatures become supra-optimal, photosynthetic rates are reduced (Prior et al. 1997; Long and Ort 2010; Yamori et al. 2014). In this perspective, leaves of C2N were significantly cooler than V + F ones (data not shown).

The proteomic comparison reported in this study also highlighted some molecular effectors that may explain the eventual performances of the citrus cybrid in facing biotic stresses and in tolerating *Phoma tracheiphila* infection (Tusa et al. 2000). In this context, worth mentioning was the over-expression in C2N proteome of peroxidase 3-like protein, an enzyme that was already associated with the biosynthesis of syringyl lignin. Accordingly, specific tolerance mechanisms to *Phoma* may be activated in the cybrid due to the increase of lignin biosynthesis. Actually, it has been reported that lignin plays a crucial role in the disease tolerance of different species (Menden et al. 2007; Gayoso et al. 2010; Tronchet et al. 2010; Xu et al. 2011; Skyba et al. 2013). Indeed, a defense-induced enrichment of lignin has already been observed in wheat (Menden et al. 2007), tomato (Gayoso et al. 2010) and cotton (Xu et al. 2011). This phenomenon was related to a triggering of the activities of peroxidase and phenylalanine-ammonia lyase (PAL); the latter enzyme is involved in phenylpropanoid metabolism and biosynthesis of lignin (Huang et al. 2010; Xu et al. 2011). In addition, lignin content contributes to mechanical support and water transport in the leaf and can play an important role in drought tolerance. Carins Murphy et al. (2016) have highlighted the relationship between leaf lignin content and minor vein volume, showing that a substantial proportion of leaf tissue dedicated to veins ensures that the investment in the vascular system is appropriate for the photosynthetic capacity of the leaf. Genetically modified poplars with low lignin content were found to have lower g_s values, lower hydraulic conductivity and greater vulnerability to cavitation (Coleman et al. 2008; Voelker et al. 2011). Since the rigidity and compression resistance of xylem elements are due to lignin deposition, which has been shown to increase under drought conditions (Lee et al. 2007), higher lignin content could increase hydraulic conductivity of the leaves and allow the tolerance of higher tensions within veins, a trait that is particularly relevant to maintain water transport under high evaporative demand. In low-lignin transgenic poplars it was observed a significant decrease in photosynthesis, which could be explained by a negative feedback mechanism due to the accumulation of carbohydrates not removed by lignin biosynthesis (Coleman et al. 2008; Marchin et al. 2017). Furthermore, lignin deficiency was found to interfere with the temperature-response of photosynthesis (Marchin et al. 2017).

Conclusion

This work illustrates that protein-, metabolite- and physiological-oriented approaches can be a valuable tool to investigate the impact of genome rearrangement in the genotypes obtained by protoplast fusion. These combined data provide a comprehensive picture of the molecular events characterizing the regenerated genotype and opens avenues to better understand the mechanisms underlying metabolic capacity regulation, such as oxidation process and photosynthetic capacity. Overall, the outcome of this study suggests novel insights into cellular processes that are regulated by the integration of different molecular signals from compartmentalized genomes. The knowledge of the way in which organellar activity is perceived by the nucleus and coordinated with the rest of cellular function, together with the targeted use of cybridization, may have a deep impact in citrus breeding. Primary objectives for citrus genetic improvement programs might be achieved developing alloplasmic cybrid plants capable to express specific nuclear genetic background in combination with useful organelle genomes related traits.

Acknowledgements 2D-DIGE analysis was performed using the instruments of Advanced Technologies Network (ATeN) Center at the University of Palermo, acquired in the frame of “Mediterranean Center for Human Health Advanced Biotechnologies” (Med-CHHAB) project (Project Code: PONA3_00273—Avviso MIUR D.D. n. 254/Ric del 18/05/2011). GC/MS and HPLC/MS analyses were performed with instruments acquired in the frame of the project PIASS-Platform for Agrofood Science and Safety (Project Code: PONA3_00053), Programma Operativo Nazionale Ricerca e Competitività 2007–2013. Asse I- Sostegno ai Mutamenti Strutturali Obiettivo Operativo 4.1.1.4—I azione.

Author contributions FM, TF, GG, SFDB and LA conceived and designed the experiments. TF, LA, APP, AM, EO and GR performed the experiments. SFDB, GG, AS, FC, AMP and FM supervised the experiments and wrote the manuscript. All authors discussed and interpreted results and read and approved the final manuscript.

Compliance with ethical standards

Conflict of interest The authors declare that they have no conflict of interest.

References

- Abbate L, Tusa N, Fatta Del Bosco S, Strano T, Renda A, Ruberto G (2012) Genetic improvement of citrus fruits: new somatic hybrids from *Citrus sinensis* (L.) Osb. and *Citrus limon* (L.) Burm. F. Food Res Int 48:284–290. <https://doi.org/10.1016/j.foodres.2012.04.007>
- Aleza P, Garcia-Lor A, Juarez J, Navarro L (2016) Recovery of citrus cybrid plants with diverse mitochondrial and chloroplastic genome combinations by protoplast fusion followed by in vitro shoot, root, or embryo micrografting. Plant Cell Tiss Organ Cult 126:205–217. <https://doi.org/10.1007/s11240-016-0991-8>
- Alqurashi M, Gehring C, Marondedze C (2016) Changes in the *Arabidopsis thaliana* proteome implicate cAMP in biotic and abiotic stress responses and changes in energy metabolism. Int J Mol Sci 17:852. <https://doi.org/10.3390/ijms17060852>
- Anoman AD, Muñoz-Bertomeu J, Rosa-Téllez S, Flores-Tornero M, Serrano R, Bueso E et al (2015) Plastidial glycolytic glyceraldehyde-3-phosphate dehydrogenase is an important determinant in the carbon and nitrogen metabolism of heterotrophic cells in *Arabidopsis*. Plant Physiol 169:1619–1637. <https://doi.org/10.1104/pp.15.00696>
- Audrius AZ, Andrew PB (2005) Extraction methods for analysis of citrus leaf proteins by two-dimensional gel electrophoresis. J Chromatogr A 1078:201–205. <https://doi.org/10.1016/j.chroma.2005.05.020>
- Bassene JB, Berti L, Carcouet E, Dhuique-Mayer C, Fanciullino AL, Bouffin J, Ollitrault P, Froelicher Y (2008) Influence of mitochondrial origin on fruit quality in a citrus cybrid. J Agric Food Chem 56:8635–8640. <https://doi.org/10.1021/jf801233m>
- Bassene JB, Froelicher Y, Navarro L, Ollitrault P, Ancillo G (2011) Influence of mitochondria on gene expression in a citrus cybrid. Plant Cell Rep 30:1077–1085. <https://doi.org/10.1007/s00299-011-1014-1>
- Belliard G, Vedel F, Pelletier G (1979) Mitochondrial recombination in cytoplasmic hybrids of *Nicotiana tabacum* by protoplast fusion. Nature 281:401–403. <https://doi.org/10.1038/281401a0>
- Bihn EA, Paul AL, Wang SW, Erdos GW, Ferl RJ (1997) Localization of 14-3-3 proteins in the nuclei of *Arabidopsis* and maize. Plant J 12:1439–1445. <https://doi.org/10.1046/j.1365-3113.1997.12061439.x>
- Brito A, Ramirez JE, Areche C, Sepúlveda B, Simirgiotis MJ (2014) HPLC-UV-MS profiles of phenolic compounds and antioxidant activity of fruits from three citrus species consumed in northern Chile. Molecules 19:17400–17421. <https://doi.org/10.3390/molecules191117400>
- Cabasson C, Luro F, Ollitrault P, Grosser JW (2001) Non-random inheritance of mitochondrial genomes in citrus hybrids produced by protoplast fusion. Plant Cell Rep 20:604–609. <https://doi.org/10.1007/s002990100370>
- Cai XD, Fu J, Deng XX, Guo WW (2007) Production and molecular characterization of potential seedless cybrid plants between pollen sterile satsuma mandarin and two seedy *Citrus* cultivars. Plant Cell Tiss Org 90:275–283. <https://doi.org/10.1007/s11240-007-9266-8>
- Carins Murphy MR, Jordan GJ, Brodribb TJ (2016) Cell expansion not cell differentiation predominantly co-ordinates veins and stomata within and among herbs and woody angiosperms grown under sun and shade. Ann Bot 118:1127–1138. <https://doi.org/10.1093/aob/mcw167>
- Cheng Y, Guo W, Deng X (2003) cpSSR: a new tool to analyse chloroplast genome of citrus somatic hybrids. Acta Bot Sin 45:906–909
- Cheng Y, De Vicente MC, Meng H, Guo W, Tao N, Deng X (2005) A set of primers for analyzing chloroplast DNA diversity in *Citrus* and related genera. Tree Physiol 25:661–672. <https://doi.org/10.1093/treephys/25.6.661>
- Chetouhi C, Bonhomme L, Lecomte P, Cambon F, Merlino M, Biron DG, Langin T (2015) A proteomics survey on wheat susceptibility to *Fusarium* head blight during grain development. Eur J Plant Pathol 141:407–418. <https://doi.org/10.1007/s10658-014-0552-0>
- Coleman HD, Samuels AL, Guy RD, Mansfield SD (2008) Perturbed lignification impacts tree growth in hybrid poplar—a function of sink strength, vascular integrity, and photosynthetic assimilation. Plant Physiol 148:1229–1237. <https://doi.org/10.1104/pp.108.125500>


- Condon A, Richards R, Rebetzke G, Farquhar G (2004) Breeding for high water-use efficiency. *J Exp Bot* 55:2447–2460. <https://doi.org/10.1093/jxb/erh277>
- Crafts-Brandner SJ, Salvucci ME (2000) Rubisco activase constrains the photosynthetic potential of leaves at high temperature and CO₂. *Proc Natl Acad Sci USA* 97:13430–13435. <https://doi.org/10.1073/pnas.230451497>
- Dambier D, Benyahia H, Pensabene-Bellavia G, Kacar YA, Froelicher Y, Belfalah Z, Lhou B, Handaji N, Printz B, Morillon R, Yesiloglu T, Navarro L, Ollitrault P (2011) Somatic hybridization for citrus rootstock breeding: an effective tool to solve some important issues of the Mediterranean citrus industry. *Plant Cell Rep* 30:883–900. <https://doi.org/10.1007/s00299-010-1000-z>
- De Lille JM, Sehnke PC, Ferl RJ (2001) The *Arabidopsis* 14-3-3 family of signaling regulators. *Plant Physiol* 126:35–38. <https://doi.org/10.1104/pp.126.1.35>
- Eeckhaut T, Lakshmanan PS, Deryckere D, Van Bockstaele E, Van Huylenbroeck J (2013) Progress in plant protoplast research. *Planta* 238:991–1003. <https://doi.org/10.1007/s00425-013-1936-7>
- Ehleringer JR, Cerling TE (1995) Atmospheric CO₂ and the ratio of intercellular to ambient CO₂ concentrations in plants. *Tree Physiol* 15:105–111. <https://doi.org/10.1093/treephys/15.2.105>
- Fanciullino AL, Gancel AL, Froelicher Y, Luro F, Ollitrault P, Brillouet JM (2005) Effects of nucleo-cytoplasmic interactions on leaf volatile compounds from citrus somatic diploid hybrids. *J Agric Food Chem* 53:4517–4523. <https://doi.org/10.1021/jf0502855>
- Fang YN, Zheng BB, Wang L, Yang W, Wu XM, Xu Q, Guo WW (2016) High-throughput sequencing and degradome analysis reveal altered expression of miRNAs and their targets in a male-sterile cybrid pummelo (*Citrus grandis*). *BMC Genom* 17:591. <https://doi.org/10.1186/s12864-016-2882-0>
- FAO (2017) <http://www.fao.org/3/a-i8092e.pdf>
- Farquhar GD, Ehleringer JR, Hubick KT (1989) Carbon isotope discrimination and photosynthesis. *Ann Rev Plant Biol* 40:503–537. <https://doi.org/10.1146/annurev.pp.40.060189.002443>
- Fatta Del Bosco S, Abbate L, Tusa N, Strano T, Renda A, Ruberto G (2013) Genetic improvement of *Citrus* fruits: The essential oil profiles in a *Citrus limon* backcross progeny derived from somatic hybridization. *Food Res Int* 50:344–350. <https://doi.org/10.1016/j.foodres.2012.10.041>
- Fatta Del Bosco S, Napoli E, Mercati F, Abbate L, Carimi F, Ruberto G (2017) Somatic cybridization for *Citrus*: polyphenols distribution in juices and peel essential oil composition of a diploid cybrid from Cleopatra mandarin (*Citrus reshni* Hort. Ex Tan.) and sour orange (*Citrus aurantium* L.). *Genet Resour Crop Evol* 64:261–275. <https://doi.org/10.1007/s10722-015-0348-x>
- Finnie C, Borch J, Collinge DB (1999) 14-3-3 proteins: eukaryotic regulatory proteins with many functions. *Plant Mol Biol* 40:545–554. <https://doi.org/10.1023/A:1006211014713>
- Froelicher Y, Mouhaya W, Bassene J, Costantino G, Kamiri M, Luro F, Morillon R, Ollitrault P (2011) New universal mitochondrial PCR markers reveal new information on maternal citrus phylogeny. *Tree Genet Genomes* 7:49–61. <https://doi.org/10.1007/s11295-010-0314-x>
- Fu LL, Yang XY, Zhang XL, Wang ZW, Feng CH, Liu CX, Jiang PY, Zhang JL (2009) Regeneration and identification of interspecific asymmetric somatic hybrids obtained by donor–recipient fusion in cotton. *Chin Sci Bull* 54:3035–3044. <https://doi.org/10.1007/s11434-009-0517-4>
- Fu J, Peng ZJ, Cai XD, Guo WW (2011) Regeneration and molecular characterization of interspecific somatic hybrids between satsuma mandarin and two seedy sweet oranges for scion improvement. *Plant Breed* 130:287–290. <https://doi.org/10.1111/j.1439-0523.2010.01773.x>
- Gallo G, Renzone G, Palazzotto E, Monciardini P, Arena S, Faddetta T et al (2016) Elucidating the molecular physiology of lantibiotic NAI-107 production in *Microbispora* ATCC-PTA-5024. *BMC Genom* 12:17–42. <https://doi.org/10.1186/s12864-016-2369-z>
- Gayoso C, Pomar F, Novo-Uzal E, Merino F, De Ilárduya OM (2010) The Ve-mediated resistance response of the tomato to *Verticillium dahliae* involves H₂O₂, peroxidase and lignins and drives PAL gene expression. *BMC Plant Biol* 10:232. <https://doi.org/10.1186/1471-2229-10-232>
- Greiner S, Bock R (2013) Tuning a ménage à trois: co-evolution and co-adaptation of nuclear and organellar genomes in plants. *BioEssays* 35:354–365. <https://doi.org/10.1002/bies.201200137>
- Grosser JW, Gmitter FG Jr (1990) Protoplast fusion and citrus improvement. *Plant Breed Rev* 8:339–374. <https://doi.org/10.1002/9781118061053.ch10>
- Grosser JW, Gmitter FG Jr, Tusa N, Reforgiato Recupero G, Cucinotta P (1996) Further evidence of a cybridization requirement for plant regeneration from citrus leaf protoplasts following somatic fusion. *Plant Cell Rep* 15:672–676. <https://doi.org/10.1007/BF00231922>
- Grosser JW, Gmitter FG Jr (2011) Protoplast fusion for production of tetraploids and triploids: applications for scion and rootstock breeding in citrus. *Plant Cell Tiss Org* 104:343–357. <https://doi.org/10.1007/s11240-010-9823-4>
- Grosser JW, Ollitrault P, Olivares-Fuster O (2000) Somatic hybridization in citrus: an effective tool to facilitate variety improvement. *In Vitro Cell Dev Biol-Plant* 36:434–449. <https://doi.org/10.1007/s11627-000-0080-9>
- Guo WW, Deng XX (2001) Wide somatic hybrids of citrus with its related genera and their potential in genetic improvement. *Euphytica* 118:175–183. <https://doi.org/10.1023/A:1004147208099>
- Guo WW, Prasad D, Cheng YJ, Serrano P, Deng XX, Grosser JW (2004) Targeted cybridization in citrus: transfer of satsuma cytoplasm to seedy cultivars for potential seedlessness. *Plant Cell Rep* 22:752–758. <https://doi.org/10.1007/s00299-003-0747-x>
- Guo WW, Cheng YJ, Chen CL, Deng XX (2006) Molecular analysis revealed autotetraploid, diploid and tetraploid cybrid plants regenerated from an interspecific somatic fusion in *Citrus*. *Sci Hortic* 108:162–166. <https://doi.org/10.1016/j.scienta.2006.01.021>
- Guo WW, Xiao SX, Deng XX (2013) Somatic cybrid production via protoplast fusion for citrus improvement. *Sci Hort* 163:20–26. <https://doi.org/10.1016/j.scienta.2013.07.018>
- Hijaz F, Nehela Y, Killiny N (2016) Possible role of plant volatiles in tolerance against huanglongbing in citrus. *Plant Signal Behav* 11:e1138193. <https://doi.org/10.1080/15592324.2016.1138193>
- Holopainen JK, Gershenzon J (2010) Multiple stress factors and the emission of plant VOCs. *Trends Plant Sci* 15:176–184. <https://doi.org/10.1016/j.tplants.2010.01.006>
- Hozain MI, Salvucci ME, Fokar M, Holaday AS (2010) The differential response of photosynthesis to high temperature for a boreal and temperate *Populus* species relates to differences in rubisco activation and rubisco activase properties. *Tree Physiol* 30:32–44. <https://doi.org/10.1093/treephys/tpp091>
- Huang J, Gu M, Lai Z, Fan B, Shi K, Zhou YH et al (2010) Functional analysis of the *Arabidopsis* PAL gene family in plant growth, development, and response to environmental stress. *Plant Physiol* 153:1526–1538. <https://doi.org/10.1104/pp.110.157370>
- Jacoby RP, Li L, Huang S, Lee CP, Millar AH, Taylor NL (2012) Mitochondrial composition, function and stress response in plants. *J Integr Plant Biol* 54:887–906. <https://doi.org/10.1111/j.1744-7909.2012.01177.x>
- Jannati M, Fotouhi R, Abad AP, Salehi Z (2009) Genetic diversity analysis of Iranian citrus varieties using micro satellite (SSR) based markers. *J Hortic For* 1:120–125

- Kanehisa M, Goto S (2000) KEGG: kyoto encyclopedia of genes and genomes. *Nucl Acids Res* 28:27–30. <https://doi.org/10.1093/nar/28.1.27>
- Komatsu S, Nanjo Y, Nishimura M (2013) Proteomic analysis of the flooding tolerance mechanism in mutant soybean. *J Proteom* 79:231–250. <https://doi.org/10.1016/j.jprot.2012.12.023>
- Korthout HA, De Boer AH (1994) A fusaric acid binding protein belongs to the family of 14-3-3 brain protein homologs. *Plant Cell* 6:1681–1692. <https://doi.org/10.1105/tpc.6.11.1681>
- Kosová K, Vítámvás P, Prášil IT, Renaut J (2011) Plant proteome changes under abiotic stress—contribution of proteomics studies to understanding plant stress response. *J Proteom* 74:1301–1322. <https://doi.org/10.1016/j.jprot.2011.02.006>
- Kusumi K, Hirotsuka S, Kumamaru T, Iba k (2012) Increased leaf photosynthesis caused by elevated stomatal conductance in a rice mutant deficient in SLAC1, a guard cell anion channel protein. *J Exp Bot* 63:695–709. <https://doi.org/10.1093/jxb/ers216>
- Lee BR, Kim KY, Jung WJ, Avicé JC, Ourry A, Kim TH (2007) Peroxidases and lignification in relation to the intensity of water-deficit stress in white clover (*Trifolium repens* L.). *J Exp Bot* 58:1271–1279. <https://doi.org/10.1093/jxb/erl280>
- Liang C, Tian J, Liao H (2013) Proteomics dissection of plant responses to mineral nutrient deficiency. *Proteomics* 13:624–636. <https://doi.org/10.1002/pmic.201200263>
- Liu SW, Xia GM (2014) The place of asymmetric somatic hybridization in wheat breeding. *Plant Cell Rep* 33:595–603. <https://doi.org/10.1007/s00299-013-1552-9>
- Liu B, Liu ZL, Li XW (1999) Production of a highly asymmetric somatic hybrid between rice and *Zizania latifolia* (Griseb): evidence for inter-genomic exchange. *Theor Appl Genet* 98:1099–1103. <https://doi.org/10.1007/s001220051173>
- Liu GT, Ma L, Duan W, Wang BC, Li JH, Xu HG et al (2014) Differential proteomic analysis of grapevine leaves by iTRAQ reveals responses to heat stress and subsequent recovery. *BMC Plant Biol* 14:110. <https://doi.org/10.1186/1471-2229-14-110>
- Lodhi MA, Ye GN, Weeden NF, Reisch BI (1994) A simple and efficient method for DNA extraction from grapevine cultivars and vitis species. *Plant Mol Biol Rep* 12:6–13. <https://doi.org/10.1007/BF02668658>
- Long SP, Ort DR (2010) More than taking the heat: crops and global change. *Curr Opin Plant Biol* 13:241–248. <https://doi.org/10.1016/j.pbi.2010.04.008>
- Loreto F, Schnitzler JP (2010) Abiotic stresses and induced BVOCs. *Trends Plant Sci* 15:154–166. <https://doi.org/10.1016/j.tplants.2009.12.006>
- Luo D, Xu H, Liu Z, Guo J, Li H, Chen L et al (2013) A detrimental mitochondrial-nuclear interaction causes cytoplasmic male sterility in rice. *Nat Genet* 45:573–577. <https://doi.org/10.1038/ng.2570>
- Marchin RM, Stout AT, Davis AA, King JS (2017) Transgenically altered lignin biosynthesis affects photosynthesis and water relations of field-grown *Populus trichocarpa*. *Biomass Bioenergy* 98:15–25. <https://doi.org/10.1016/j.biombioe.2017.01.013>
- Menden B, Kohlhoff M, Moerschbacher BM (2007) Wheat cells accumulate a syringyl-rich lignin during the hypersensitive resistance response. *Phytochemistry* 68:513–520. <https://doi.org/10.1016/j.phytochem.2006.11.011>
- Mercati F, Riccardi P, Leebens-Mack J, Abenavoli MR, Falavigna A, Sunseri F (2013) Single nucleotide polymorphism isolated from a novel EST dataset in garden asparagus (*Asparagus officinalis* L.). *Plant Sci* 203–204:115–123. <https://doi.org/10.1016/j.plantsci.2013.01.002>
- Miner GL, Bauerle WL, Baldocchi DD (2017) Estimating the sensitivity of stomatal conductance to photosynthesis: a review. *Plant Cell Environ* 40(7):1214–1238. <https://doi.org/10.1111/pce.12871>
- Moreira CD, Chase CD, Gmitter FG Jr, Grosser JW (2000) Inheritance of organelle genomes in citrus somatic cybrids. *Mol Breeding* 6:401–405. <https://doi.org/10.1023/A:1009632223708>
- Muñoz-Bertomeu J, Cascales-Miñana B, Alaiiz M, Segura J, Ros R (2010) A critical role of plastidial glycolytic glyceraldehyde-3-phosphate dehydrogenase in the control of plant metabolism and development. *Plant Signal Behav* 5:67–69. <https://doi.org/10.4161/psb.5.1.10200>
- Muñoz-Bertomeu J, Bermudez MA, Segura J, Ros R (2011) *Arabidopsis* plants deficient in plastidial glyceraldehyde-3-phosphate dehydrogenase show alterations in abscisic acid (ABA) signal transduction: interaction between ABA and primary metabolism. *J Exp Bot* 62:1229–1239. <https://doi.org/10.1093/jxb/erq353>
- Navarro L, Aleza P, Cuenca J, Juárez J, Pina JA, Ortega C, Navarro A, Ortega V (2015) The mandarin triploid breeding program in Spain. *Acta Hort* 1065:389–396. <https://doi.org/10.17660/ActaHortic.2015.1065.48>
- Ng S, De Clercq I, Van Aken O, Law SR, Ivanova A, Willems P et al (2014) Anterograde and retrograde regulation of nuclear genes encoding mitochondrial proteins during growth, development, and stress. *Mol Plant* 7:1075–1093. <https://doi.org/10.1093/mp/ssu037>
- Oecking C, Eckerskornb C, Weiler EW (1994) The fusaric acid receptor of plants is a member of the 14-3-3 superfamily of eukaryotic regulatory proteins. *FEBS Lett* 352:163–166. [https://doi.org/10.1016/0014-5793\(94\)00949-X](https://doi.org/10.1016/0014-5793(94)00949-X)
- Omar AA, Murata M, Yu Q, Gmitter FG Jr, Chase CD, James H, Graham JH, Grosser JW (2017) Production of three new grapefruit cybrids with potential for improved citrus canker resistance. *In Vitro Cell Dev Biol—Plant* 53:256–269. <https://doi.org/10.1007/s11627-017-9816-7>
- Osborn TC, Pires JC, Birchler JA, Auger DL, Chen ZJ, Lee HS, Comai L, Madlung A, Doerge RW, Colot V, Martienssen RA (2003) Understanding mechanisms of novel gene expression in polyploids. *Trends Genet* 19:141–147. [https://doi.org/10.1016/S0168-9525\(03\)00015-5](https://doi.org/10.1016/S0168-9525(03)00015-5)
- Palazzotto E, Renzone G, Fontana P, Botta L, Scaloni A, Puglia AM, Gallo G (2015) Tryptophan promotes morphological and physiological differentiation in *Streptomyces coelicolor*. *Appl Microbiol Biotechnol* 99:10177–10189. <https://doi.org/10.1007/s00253-015-7012-4>
- Palazzotto E, Gallo G, Renzone G, Giardina A, Sutura A, Silva J, Vocat C, Botta L, Scaloni A, Puglia AM (2016) TrpM, a small protein modulating tryptophan biosynthesis and morpho-physiological differentiation in *Streptomyces coelicolor* A3(2). *PLoS ONE* 11(9):e0163422. <https://doi.org/10.1371/journal.pone.0163422>
- Palma JM, Corpas FJ, Del Río LA (2011) Proteomics as an approach to the understanding of the molecular physiology of fruit development and ripening. *J Proteom* 74:1230–1243. <https://doi.org/10.1016/j.jprot.2011.04.010>
- Penuelas J, Llusà J (2002) Linking photorespiration, monoterpenes and thermotolerance in *Quercus*. *New Phytol* 155:227–237. <https://doi.org/10.1046/j.1469-8137.2002.00457.x>
- Penuelas J, Munne-Bosch S (2005) Isoprenoids: an evolutionary pool for photoprotection. *Trends Plant Sci* 10:166–169. <https://doi.org/10.1016/j.tplants.2005.02.005>
- Pollock SV, Colombo SL, Prout DL Jr, Godfrey AC, Moroney JV (2003) Rubisco activase is required for optimal photosynthesis in the green alga *Chlamydomonas reinhardtii* in a low-CO₂ atmosphere. *Plant Physiol* 133:1854–1861. <https://doi.org/10.1104/pp.103.032078>
- Portis AR Jr, Li C, Wang D, Salvucci ME (2008) Regulation of rubisco activase and its interaction with rubisco. *J Exp Bot* 59:1597–1604. <https://doi.org/10.1093/jxb/erm240>
- Prior LD, Eamus D, Duff GA (1997) Seasonal and diurnal patterns of carbon assimilation, stomatal conductance and leaf water

- potential in *Eucalyptus tetrodonta* saplings in a wet-dry savanna in northern Australia. *Aust J Bot* 45:241–258. <https://doi.org/10.1071/BT96017>
- Puglia AM, Vohradsky J, Thompson CJ (1995) Developmental control of the heat-shock stress regulon in *Streptomyces coelicolor*. *Mol Microbiol* 17:737–746. https://doi.org/10.1111/j.1365-2958.1995.mmi_17040737.x
- Rampitsch C, Bykova NV (2012) Proteomics and plant disease: advances in combating a major threat to the global food supply. *Proteomics* 12:673–690. <https://doi.org/10.1002/pmic.201100359>
- Rolland N, Curien G, Finazzi G, Kuntz M, Maréchal E, Matringe M et al (2012) The biosynthetic capacities of the plastids and integration between cytoplasmic and chloroplast processes. *Annu Rev Genet* 46:233–264. <https://doi.org/10.1146/annurev-genet-110410-132544>
- Roose JL, Frankel LK, Bricker TM (2010) Documentation of significant electron transport defects on the reducing side of photosystem II upon removal of the PsbP and PsbQ extrinsic proteins. *Biochemistry* 49:36–41. <https://doi.org/10.1021/bi9017818>
- Rott M, Martins NF, Thiele W, Lein W, Bock R, Kramer DM, Schotler MA (2011) ATP synthase repression in tobacco restricts photosynthetic electron transport, CO₂ assimilation, and plant growth by overacidification of the thylakoid lumen. *Plant Cell* 23:304–321. <https://doi.org/10.1105/tpc.110.079111>
- Salvucci ME (2008) Association of rubisco activase with chaperonin-60b: a possible mechanism for protecting photosynthesis during heat stress. *J Exp Bot* 59:1923–1933. <https://doi.org/10.1093/jxb/erm343>
- Saravanan RS, Rose JKC (2004) A critical evaluation of sample extraction techniques for enhanced proteomic analysis of recalcitrant plant tissues. *Proteomics* 4:2522–2532. <https://doi.org/10.1002/pmic.200300789>
- Satpute AD, Chen C, Gmitter FG Jr, Ling P, YU Q, Grosser MR, Chase CD, Grosser JW (2015) Cybridization of grapefruit with “Dancy” mandarin leads to improved fruit characteristics. *J Am Soc Hortic Sci* 140(5):427–435
- Scarano MT, Tusa N, Abbate L, Lucretti S, Nardi L, Ferrante S (2003) Flow cytometry, SSR and modified AFLP markers for the identification of zygotic plantlets in backcrosses between ‘femminello’ lemon cybrids (2n and 4n) and a diploid clone of ‘femminello’ lemon (*Citrus limon* L. Burm. F.) tolerant to mal secco disease. *Plant Sci* 164:1009–1017. [https://doi.org/10.1016/S0168-9452\(03\)00088-8](https://doi.org/10.1016/S0168-9452(03)00088-8)
- Sehnke PC, Ferl RJ (2000) Plant 14-3-3s: omnipotent metabolic phosphopartners. *Science’s STKE* 56:1–3. <https://doi.org/10.1126/stke.2000.56.pe1>
- Sehnke PC, Henry R, Cline K, Ferl RJ (2000) Interaction of a plant 14-3-3 protein with the signal peptide of a thylakoid-targeted chloroplast precursor protein and the presence of 14-3-3 isoforms in the chloroplast stroma. *Plant Physiol* 122:235–242. <https://doi.org/10.1104/pp.122.1.235>
- Sehnke PC, Chung HJ, Wu K, Ferl RJ (2001) Regulation of starch accumulation by granule-associated plant 14-3-3 proteins. *Proc Natl Acad Sci USA* 98:765–770. <https://doi.org/10.1073/pnas.98.2.765>
- Sharkey TD, Raschke K (1981) Separation and measurement of direct and indirect effects of light on stomata. *Plant Physiol* 68:33–40. <https://doi.org/10.1104/pp.68.1.33>
- Skyba O, Douglas CJ, Mansfield SD (2013) Syringyl-rich lignin renders poplars more resistant to degradation by wood decay fungi. *Appl Environ Microbiol* 79:2560–2571. <https://doi.org/10.1128/AEM.03182-12>
- Sparkman O (2005) Identification of essential oil components by gas chromatography/quadrupole mass spectroscopy Robert P. Adams. *J Am Soc Mass Spectrom* 16(11):1902–1903. <https://doi.org/10.1016/j.jasms.2005.07.008>
- Suzuki N, Koussevitzky S, Mittler R, Miller G (2012) ROS and redox signalling in the response of plants to abiotic stress. *Plant Cell Environ* 35:259–270. <https://doi.org/10.1111/j.1365-3040.2011.02336.x>
- Tarwacka J, Polkowska-Kowalczyk L, Kolano B, Sliwka J, Wielgat B (2013) Interspecific somatic hybrids *Solanum villosum* (+) *S. tuberosum*, resistant to *Phytophthora infestans*. *J Plant Physiol* 170:1541–1548. <https://doi.org/10.1016/j.jplph.2013.06.013>
- Tezara W, Coronel I, Herrera A, Dzib G, Canul-Puc K, Calvo-Irabién LM, González-Meler M (2014) Photosynthetic capacity and terpene production in populations of *Lippia graveolens* (Mexican oregano) growing wild and in a common garden in the Yucatán peninsula. *Ind Crop Prod* 57:1–9. <https://doi.org/10.1016/j.indcrop.2014.03.012>
- Tronchet M, Balagué C, Kroj T, Jouanin L, Roby D (2010) Cinnamyl alcohol dehydrogenases-C and D, key enzymes in lignin biosynthesis, play an essential role in disease resistance in *Arabidopsis*. *Mol Plant Pathol* 11:83–92. <https://doi.org/10.1111/j.1364-3703.2009.00578.x>
- Tusa N, Grosser JW, Gmitter FG Jr (1990) Plant regeneration of ‘Valencia’ sweet orange, ‘femminello’ lemon, and the interspecific somatic hybrid following protoplast fusion. *J Am Soc Hortic Sci* 115:1043–1046
- Tusa N, Fatta Del Bosco S, Nigro F, Ippolito A (2000) Response of cybrids and a somatic hybrid of Lemon to *Phoma tracheiphila* infections. *Hort Science* 35:125–127
- Vedel F, Chétrit P, Mathieu C, Pelletier G, Primard C (1986) Several different mitochondrial DNA regions are involved in intergenomic recombination in *Brassica napus* cybrid plants. *Curr Genet* 11:17–24. <https://doi.org/10.1007/BF00389421>
- Visioli G, Marmioli N (2013) The proteomics of heavy metal hyperaccumulation by plants. *J Proteom* 79:133–145. <https://doi.org/10.1016/j.jprot.2012.12.006>
- Voelker SL, Lachenbruch B, Meinzer FC, Kitin P, Strauss SH (2011) Transgenic poplars with reduced lignin show impaired xylem conductivity, growth efficiency and survival. *Plant Cell Environ* 34:655–668. <https://doi.org/10.1111/j.1365-3040.2010.02270.x>
- Wang W, Vignani R, Scali M, Cresti M (2006) A universal and rapid protocol for protein extraction from recalcitrant plant tissues for proteomic analysis. *Electrophoresis* 27:2782–2786. <https://doi.org/10.1002/elps.200500722>
- Wang L, Pan Z-Y, Guo WW (2010) Proteomic analysis of leaves from a diploid cybrid produced by protoplast fusion between Satsuma mandarin and pummelo. *Plant Cell Tissue Organ Cult* 103:165–174. <https://doi.org/10.1007/s11240-010-9764-y>
- Willer H, Lernoud J (2016) The world of organic agriculture. Statistics and emerging trends 2016, 17th edn. Research Institute of Organic Agriculture FiBL and IFOAM Organics International, Frick, Bonn
- Wong SC, Cowan IR, Farquhar GD (1979) Stomatal conductance correlates with photosynthetic capacity. *Nature* 282:424–426. <https://doi.org/10.1038/282424a0>
- Woodson JD, Chory J (2008) Coordination of gene expression between organellar and nuclear genomes. *Nat Rev Genet* 9:383–395. <https://doi.org/10.1038/nrg2348>
- Xiao SX, Biswas MK, Li MY, Deng XX, Xu Q, Guo WW (2014) Production and molecular characterization of diploid and tetraploid somatic cybrid plants between male sterile satsuma mandarin and seedy sweet orange cultivars. *Plant Cell Tissue Organ Cult* 116:81–88. <https://doi.org/10.1007/s11240-013-0384-1>
- Xu L, Zhu L, Tu L, Liu L, Yuan D, Jin L et al (2011) Lignin metabolism has a central role in the resistance of cotton to the wilt fungus *Verticillium dahliae* as revealed by RNA-Seq-dependent

- transcriptional analysis and histochemistry. *J Exp Bot* 62:5607–5621. <https://doi.org/10.1093/jxb/err245>
- Yamori W, Takahashi S, Makino A, Price GD, Badger MR, Von Caemmerer S (2011) The roles of ATP synthase and the cytochrome b6/f complexes in limiting chloroplast electron transport and determining photosynthetic capacity. *Plant Physiol* 155:956–962. <https://doi.org/10.1104/pp.110.168435>
- Yamori W, Hikosaka K, Way DA (2014) Temperature response of photosynthesis in C3, C4, and CAM plants: temperature acclimation and temperature adaptation. *Photosynth Res* 119:101–117. <https://doi.org/10.1007/s11120-013-9874-6>
- Zhang Y, Xu L, Zhu X, Gong Y, Xiang F, Sun X, Liu L (2013) Proteomic analysis of heat stress response in leaves of Radish (*Raphanus sativus* L.). *Plant Mol Biol Rep* 31:195–203. <https://doi.org/10.1007/s11105-012-0486-7>
- Zhao Q, Zhanga H, Wang T, Chen S, Daia S (2013) Proteomics-based investigation of salt-responsive mechanisms in plant roots. *J Proteom* 82:230–253. <https://doi.org/10.1016/j.jprot.2013.01.024>
- Zheng BB, Wu XM, Ge XX, Deng XX, Grosser JW, Guo WW (2012) Comparative transcript profiling of a male sterile cybrid pummelo and its fertile type revealed altered gene expression related to floral organ development. *PLoS ONE* 7(8):e43758. <https://doi.org/10.1371/journal.pone.0043758>
- Zheng BB, Fang YN, Pan ZY, Sun L, Deng XX, Grosser JW, Guo WW (2014) iTRAQ based quantitative proteomics analysis revealed alterations of carbohydrate metabolism pathways and mitochondrial proteins in a male sterile cybrid pummelo. *J Proteome Res* 13:2998–3015. <https://doi.org/10.1021/pr500126g>

Affiliations

Teresa Faddetta^{1,2} · Loredana Abbate³ · Giovanni Renzone⁴ · Antonio Palumbo Piccionello¹ · Antonella Maggio¹ · Elisabetta Oddo¹ · Andrea Scaloni⁴ · Anna Maria Puglia¹ · Giuseppe Gallo^{1,2} · Francesco Carimi³ · Sergio Fatta Del Bosco³ · Francesco Mercati³ 

Teresa Faddetta
teresa.faddetta@unipa.it

Loredana Abbate
loredana.abbate@ibbr.cnr.it

Giovanni Renzone
giovanni.renzone@ispaam.cnr.it

Antonio Palumbo Piccionello
antonio.palumbopiccionello@unipa.it

Antonella Maggio
antonella.maggio@unipa.it

Elisabetta Oddo
elisabetta.oddo@unipa.it

Andrea Scaloni
andrea.scaloni@ispaam.cnr.it

Anna Maria Puglia
a.maria.puglia@unipa.it

Giuseppe Gallo
giuseppe.gallo@unipa.it

Francesco Carimi
francesco.carimi@ibbr.cnr.it

Sergio Fatta Del Bosco
sergio.fatta@ibbr.cnr.it

¹ Department of Biological, Chemical and Pharmaceutical Sciences and Technologies (STEBICEF), University of Palermo, Palermo, Italy

² Advanced Technologies Network (ATeN) Center, University of Palermo, Palermo, Italy

³ Institute of Biosciences and Bioresources (IBBR), National Research Council, Palermo, Italy

⁴ Proteomics & Mass Spectrometry Laboratory, ISPAAM, National Research Council, Naples, Italy